J. Min. Metall. Sect. B-Metall. 49 (1) B (2013) 13 - 20

Journal of Mining and Metallurgy, Section B: Metallurgy

REDUCTION OF Fe AND Ni IN Fe-Ni-O SYSTEMS

Y. Zhang[a], W. Wei[a,*], X. Yang[a], F.Wei[a]

[a] State Key Laboratory of Advanced Metallurgy, University of Science and Technology Beijing, Beijing 100083, China

(Received 08 February 2012; accepted 22 October 2012)

Abstract

The reduction behaviors of Fe-Ni-O compounds/systems (NiO, Fe_2O_3, $NiFe_2O_4$, Fe_2O_3 + NiO and Fe_2O_3 + Ni) were studied using H_2 and activated carbon C as reducing agents, and the mechanism of $NiFe_2O_4$ reduction was analyzed. With H_2 as reductant, these systems showed lower starting reaction temperatures and lower reaction rates. The differences of reaction rates among the different samples were small compared to those using C as reductant. With C as reductant, the reduction of the Fe_2O_3 + NiO system was much more facile compared to $NiFe_2O_4$, Fe_2O_3 + Ni, and pure Fe_2O_3. The heat released from the initial reduction of NiO by CO led to a higher temperature, which was more favorable for the further reduction of the Fe_2O_3 + NiO system. In both cases, $NiFe_2O_4$ appeared to be more difficult to reduce, as it required a higher starting temperature and exhibited a lower reaction rate and lower final reduction degree. Additionally, the data suggested that with increasing temperature, the products for the reduction of $NiFe_2O_4$ appeared in the order $NiFe_2O_4 \rightarrow Fe_3O_4$ + NiO $\rightarrow Fe_3O_4$ + Ni $\rightarrow$ FeO + $Fe_xNi_y \rightarrow Fe_xNi_y$ + Fe (Fe_mC_n). Based on this data, kinetic information about the H_2 reduction for the five compounds/systems, such as apparent activation energy and reaction mechanism, was obtained.

Keywords: Fe-Ni-O system; H_2; Activated carbon; Reduction behavior; Kinetics.

1. Introduction

In recent years, the stainless steel industry has developed rapidly in China, and as a consequence, a large amount of stainless steel dust has been generated. Generally, 18–30 $kg \cdot t^{-1}$ (steel) dust is produced during the stainless steel-making process, in which the contents of Fe, Cr and Ni are 40–60%, 8–15% and 3–9%, respectively [1–3]. High-grade Ni/Cr-bearing resources are very expensive. Based on the current conditions for stainless steel production in China, a rough estimate showed that raw material costs constituted nearly half of the total cost. Therefore, the effective recovery of Ni/Cr from the dust is of great importance. On the other hand, generally in Ni-bearing ores such as laterite, Ni is also coexisted with Fe (the total Fe (%) in laterite is about 30% [4]). In order to effectively utilize such kinds of resources, a better understanding of the reduction behaviors of Ni-Fe-O systems and their interactive influence is necessary.

The non-isothermal hydrogen reduction of nickel oxide, synthesized by the sol-gel procedure, was investigated by Jankovic [5]. The apparent activation energy E_a was 90.8 $kJ \cdot mol^{-1}$, the logarithm of the frequency factor was 19.5 min^{-1}, and the kinetic equation was $f(\alpha) = \alpha^{0.63}(1-\alpha)^{1.39}$, in which α was the reduction degree. Sharma et al. [6–7] investigated the interaction of micron-sized nickel oxide particles with pieces of stress-recrystallized pyrolytic graphite between 950 and 1000°C. Microscopic results suggested that reaction took place only at activated sites, and the nickel produced in the reduction reaction coated the NiO with a sintered layer.

With both H_2 and activated carbon (C) as reductants, previous investigations [8–11] have shown that the reaction path for Fe_2O_3 was as follows: $Fe_2O_3 \rightarrow Fe_3O_4 \rightarrow FeO \rightarrow Fe$, according to the theory of Gradual Deoxidizing. Morphological study confirmed the formation of a compact iron layer during the reduction of Fe_2O_3 by H_2 at temperatures higher than 420°C [8]. A study in which $NiFe_2O_4$ was prepared at 1000–1200°C and reduced by hydrogen at 900–1100°C [12] reported an incomplete reduction (about 80%), which was attributed to the formation of a dense metallic layer (Fe_xNi_y) surrounding the wustite layer which prevented the further diffusion of the reduction gas. The data suggested that at temperatures between 1000 and 1100°C, the initial $NiFe_2O_4$ reduction rate was mix-controlled by gaseous diffusion and interfacial chemical reaction, while in the final stage, the interfacial chemical reaction was

* *Corresponding author: weiwenjie_99@163.com*

DOI:10.2298/JMMB120208038Z

the rate-controlling step. At 1200°C, the initial rate-controlling step was the interfacial chemical reaction, while solid-state diffusion was the rate-controlling step in the final stages.

In this paper, the reduction behaviors of five oxide systems (NiO, Fe_2O_3, $NiFe_2O_4$, Fe_2O_3 + NiO and Fe_2O_3 + Ni) were studied using H_2 and C as reducing agents. The mechanism of $NiFe_2O_4$ reduction (the primary form of Ni in stainless steel dust [13]) and the products obtained at different temperatures were analyzed with the aid of X-ray diffractometry (XRD). Based on the experimental data, kinetic information, such as activation energy and reaction mechanism, was obtained.

2. Experimental

2.1 Materials

NiO, Fe_2O_3, Ni and activated carbon powder were employed in the experiments. The purities of these materials are AR. H_2 (99%) and activated carbon powder (C) were used as reductants. Ceramic crucibles, which were outfitted with the thermal analyzers, were used in non-isothermal experiments, and alumina crucibles were used in isothermal experiments.$NiFe_2O_4$ was prepared by heating a mixture of NiO and Fe_2O_3 (molar ratio 1:1) at 900°C for 8 h in a resistance furnace. XRD patterns of the product agreed well with the referred one, and are shown in Fig. 1. The results strongly suggested that high purity $NiFe_2O_4$ was obtained, which was used in the subsequent experiments.

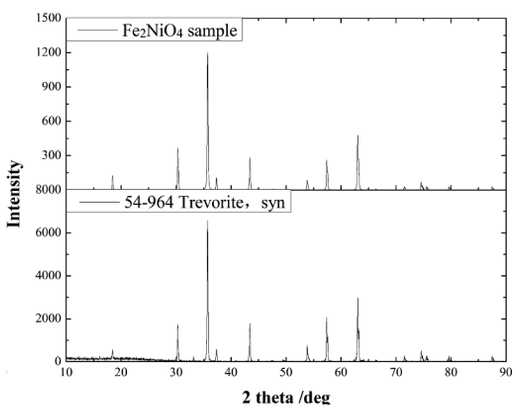

Figure 1. *XRD patterns for $NiFe_2O_4$*

2.2 Apparatus

For reductions using C, non-isothermal tests were carried out in a different integrated thermal analyzer (STA409C, NETZSCH Scientific Instruments, Germany). And for reductions with H_2, non-isothermal reduction tests were carried out in an integrated thermal analyzer (HTC-2, Beijing Hengjiu Instrument Ltd., China).

In order to obtain detailed information about the reaction mechanism of $NiFe_2O_4$ reduction, isothermal experiments were performed at five operating temperatures (450, 500, 550, 600 and 700°C) in a resistance furnace (shown as Fig.2, made by Baotou Agile Furnace, China).

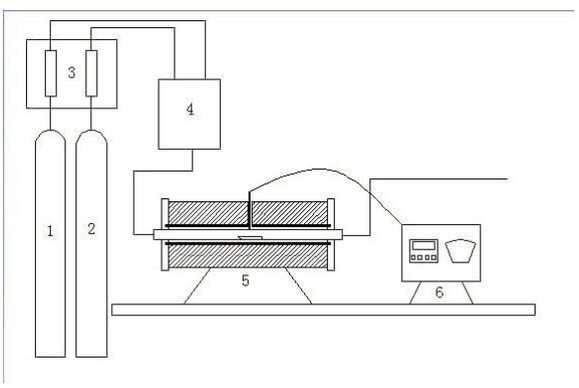

Figure 2. *Resistance furnace schematic diagram: 1–nitrogen source; 2–hydrogen source; 3–flow meters; 4–gas mixing chamber; 5–resistance furnace; 6–control cabinet.*

2.3 Experiment program

Experiment program are shown in Table 1 and 2. The molar ratio of elements of Fe and Ni in these complex sample is always 2:1. In experiments for reduction with C, C content is 30% and the protective atmosphere is Ar with flow of 30ml/min. In TG experiments for reduction with H_2, the flow of H_2 is 40ml/min. For isothermal experiments, the reduction atmosphere are H_2 (1L/min) and N_2 (2L/min).

The values of heating rates in experiments are in the range of normal heating rate of the instruments. Therefore, there is no influence of the heating rate on reduction temperatures.

2.4 Analysis

2.4.1 Reduction degree

The reduction degree (α) of the sample reduced by H_2 and C can be expressed as Eq.(1) and (2), respectively. And, in the case of using C the formation of CO_2 was ignored.

$$\alpha = \frac{m_i - m_t}{m_O} \tag{1}$$

$$\alpha = \frac{16(m_i - m_t)}{28 m_O} \tag{2}$$

where, α is the reduction degree (%); m_i is the initial mass of the sample (mg); m_t is an actual mass

Table 1. *non-isothermal experimental conditions*

Run No.	Sample	Mass of sample (g)	Reduction temperature (°C)	Reduction time (min)
HB-1	$NiFe_2O_4$	3.004	450	20
HB-2	$NiFe_2O_4$	3.001	500	20
HB-3	$NiFe_2O_4$	3.002	550	20
HB-4	$NiFe_2O_4$	3.002	600	20
HB-5	$NiFe_2O_4$	3	650	20
HB-6	$NiFe_2O_4$	2.999	700	20

Table 2. *Isothermal experimental conditions*

Run No.	Sample	Mass of sample (mg)	Heating rate (°C·min^{-1})	Final temperature (°C)
CA-1	C + NiO	15.03	10	900
CA-2	C + Fe_2O_3	15	10	1100
CA-3	C + NiO + Fe_2O_3	15.02	10	1000
CA-4	C + $NiFe_2O_4$	15.04	10	1100
CA-5	C + Ni + Fe_2O_3	15	10	1100
CB-1	C + NiO + Fe_2O_3	15.01	10	750
CB-1	C + $NiFe_2O_4$	15.02	10	895
CB-1	C + $NiFe_2O_4$	15.01	10	938
CB-1	C + Ni + Fe_2O_3	15.02	10	890
HA-1	NiO	30.3	10	700
HA-2	NiO	30.3	15	700
HA-3	NiO	30	20	700
HA-4	$NiFe_2O_4$	30.4	10	1000
HA-5	$NiFe_2O_4$	30.1	15	1000
HA-6	$NiFe_2O_4$	30.4	20	1000
HA-7	Fe_2O_3	30.4	10	1000
HA-8	Fe_2O_3	30.3	20	1000
HA-9	Fe_2O_3 + NiO	30	10	1000
HA-10	Fe_2O_3 + NiO	30	15	1000
HA-11	Fe_2O_3 + NiO	30.1	20	1000
HA-12	Fe_2O_3 + Ni	30.3	10	1000

at time t (mg); and m_O is the total content of oxygen in the initial sample (mg).

2.4.2 Activation energy and reaction mechanism

The apparent activation energy of the reduction process under non-isothermal conditions can be calculated by the Kissinger-Akahira-Sunose (KAS) method [4], which follows from the logarithmic form of Eq. (3):

$$\ln(\frac{\beta}{T^2}) = \ln[\frac{AR}{E_a g(\alpha)}] - \frac{E_a}{RT} \quad (3)$$

where, β, T, and A represent the heating rate (K·min^{-1}), temperature (K), and frequency factor (s^{-1}), respectively; R, E_a, and $g(\alpha)$ are the gas constant (8.314 J·(mol·K)$^{-1}$), activation energy (J·mol^{-1}), and the integral form of the reaction model, respectively. E_a could be calculated by iso-conversional method.

If the integral form of the mechanism shows a linear relationship with time based on the experimental data, then the corresponding function would be the rate-controlling mechanism.

3. Results and Discussion

3.1 Differences with H_2 and C as reductants

The curves obtained from thermogravimetry (TG) tests for the three systems ($NiFe_2O_4$, Fe_2O_3 + NiO and Fe_2O_3 + Ni), including reduction degrees and instantaneous rates with temperature increases, are shown in Figs. 3–5. T_i and T_f represent the extrapolated initial and final temperatures, respectively. Several peaks appear in instantaneous

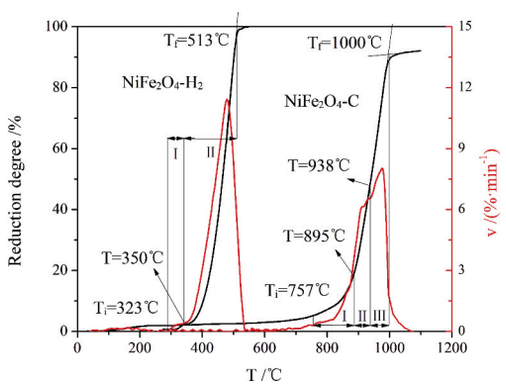

Figure 3. *Evolution of reduction degree and instantaneous rate vs. temperature for $NiFe_2O_4$*

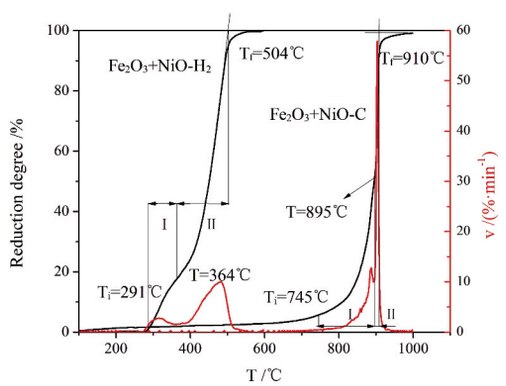

Figure 4. *Evolution of reduction degree and instantaneous rate vs. temperature for Fe_2O_3 + NiO*

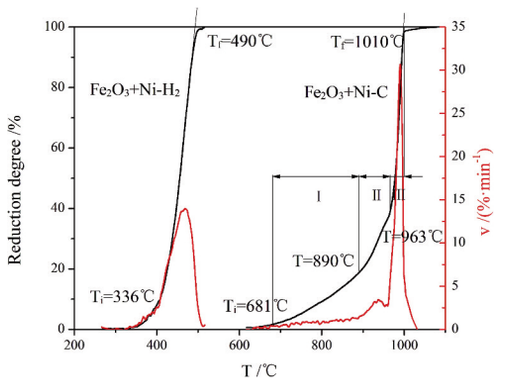

Figure 5. *Evolution of reduction degree and instantaneous rate vs. temperature for Fe_2O_3 + Ni*

rate curve.

The data in Figs. 3-5 suggested that reduction in these three systems could be enhanced by H_2, as compared to C. The H_2 reduction temperatures were much lower. For example, the T_f for NiO, Fe_2O_3 and $NiFe_2O_4$ reduced by H_2 were 602, 520 and 513°C, respectively, while T_f for those reductions using C were 783, 1017 and 1000°C, respectively. Moreover, higher reduction degrees were obtained when using H_2. The reduction degrees of all three oxide systems reduced by H_2 reached 100%, while those of $NiFe_2O_4$ and Fe_2O_3 + NiO reduced by C were 92.1 and 99.2%, respectively. A possible explanation for this lower relative reduction degree could be that the solid-solid reaction took place only at activated sites, while the metal produced in the reduction reaction covered the unreacted oxide with a sintered layer, resulting in less favorable conditions for kinetic control of the reaction [5–6, 9]. Furthermore, the differences in the reaction rates among the three systems were much smaller in the case of H_2 compared with that of C. The maximum reaction rates for Fe_2O_3 + NiO and Fe_2O_3 + Ni with C were 57.9 and 30.0%·min^{-1}, which were much higher than the rates of 9.7 and 13.6%·min^{-1} obtained with H_2, respectively. This could be due to the higher temperature at which the reduction by C was performed.

3.2 Differences among the five systems

The reduction curves (heating rate: 10°C·min^{-1}) for the five systems reduced by C and H_2 are shown in Fig.6 and Fig.7, respectively. The reduction degrees and reaction rates for the five systems showed variable dependence on temperature.

With C as reductant(Fig.6), the release of Ni from $NiFe_2O_4$ was more difficult than from NiO, while the reduction of Fe from $NiFe_2O_4$ was easier than from Fe_2O_3. For the three mixed Fe and Ni systems (Fe_2O_3 + NiO, Fe_2O_3 + Ni and $NiFe_2O_4$), Fe_2O_3 + NiO was obviously the most easily reduced, with the lowest

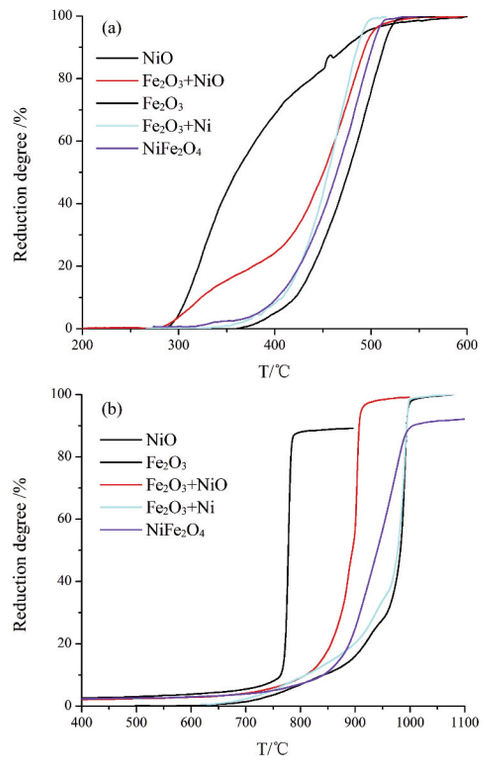

Figure 6. *Reduction degree (a) and rate curves (b) for the five systems by C.*

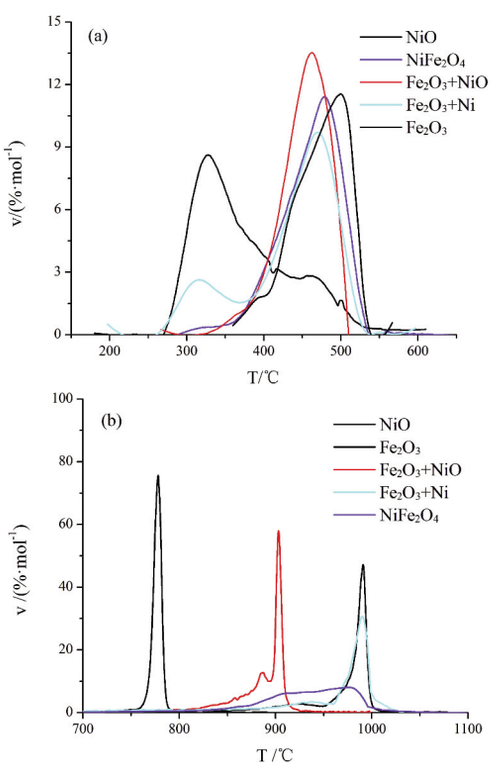

Figure 7. *Reduction degree (a) and rate curves (b) for the five systems by H_2.*

temperature for starting reaction, lowest temperature for reaching the final reduction degree (Fig. 6a), and lowest temperature corresponding to the maximum reaction rate (Fig. 6b). This is partly because the CO formed in the early stage through NiO reduction by C will promote the reduction of Fe_2O_3. More importantly, the reduction of NiO by CO is strongly exothermic, the heat released in the early stage leads to a rapid increase in the local temperature of the sample, and then it will promote the further reduction. It has to be noted that thermodynamically the production of metallic Ni (from NiO) in the sample will decrease the activity of Fe (due to the possible formation of Fe-Ni alloy), and then it also can promote the reduction of Fe_2O_3 in the sample of Fe_2O_3 + NiO. However, Fig.6 suggested that Fe_2O_3 and Fe_2O_3 + Ni showed very similar reduction behavior revealing that this effect does not predominate.

Similarly, in the study of Fe-Cr-O reduction using C as reductant by Wei [13], it was observed that under the same conditions (1550°C, 1 h), the total reduction degree of Fe_2O_3 + Cr_2O_3 was much higher than that of $FeCr_2O_4$. Considering that, thermodynamically, Cr_2O_3 cannot react with CO at 1550°C, the heat released through the reduction of Fe_2O_3 in the early stage is responsible for promoting the reduction of Cr in the later stage. Additionally, Fig.6 suggested that compared with Fe_2O_3 + NiO and Fe_2O_3 + Ni, both of the final reduction degree and reaction rate of $NiFe_2O_4$ is much lower, suggesting that $NiFe_2O_4$ is the most difficult to be reduced. Another possible explanation for lower final reduction degree in both of NiO and $NiFe_2O_4$ samples may be attributed to the formation of a dense metallic layer (Ni/Fe_xNi_y) coating the unreacted layer which kinetically limited the further reaction, as previously reported by literature [6, 7, 10].

On the other hand, in the case of H_2 as reductant (Fig.7), both of the final reduction degree and the temperature corresponding to the maximum reduction rate showed extremely small difference among the three Fe-Ni-O system: Fe_2O_3+Ni, Fe_2O_3+NiO and $NiFe_2O_4$. And the temperature corresponding to the maximum reaction rate of the three Fe-Ni-O system (Fig.7b) slightly decreased in the order: $NiFe_2O_4$> Fe_2O_3+NiO>Fe_2O_3+Ni. It tends to suggested that Fe in the Fe_2O_3 + Ni system appeared to be more easily reduced than from NiO + Fe_2O_3 system, which may be explained by the reaction of NiO+H_2 is endothermic. Anyway, compared with the case of using C as reductant, the difference among different samples is much smaller.

3.3 Discuss on the reduction process of $NiFe_2O_4$

Further studies were carried out to understand the process of $NiFe_2O_4$ reduction. Fig. 8(a) and (b) show the XRD (M21X super power X-ray diffraction made by Mac Science of Japan) patterns of the products obtained at different temperatures by using of C and H_2 as reductants, respectively.

As shown in Fig.8(a), in the reduction of $NiFe_2O_4$ by C, Fe_3O_4 and a single Ni substance were the first products at 895°C, and the corresponding reduction degree was 18.6%; At 938°C, Fe_3O_4 and Ni had disappeared, and FeO and Fe-Ni alloy (mainly in the form of $FeNi_3$) were present; At 1100°C, the oxides were completely reduced, and the main products were Fe-Ni alloy and iron carbide.

In the case of H_2 as reductant (Fig.8(b)), Fe_3O_4 was the first reduction product. Then, Ni was gradually released with increasing temperature, and combined with the produced Fe to form different Fe-Ni alloys.

There were two differences between the reduction processes of $NiFe_2O_4$ by H_2 and C. First, FeO was absent during reduction process by H_2, which is attributable to the low reduction temperature. Second, the form of Fe-Ni alloy was also different(for example, using C as redutant $FeNi_3$ was observed, while in the case of H_2 $Fe_{0.64}Ni_{0.36}$ was present). One reason was the change in reduction temperature, and the other was the different Fe/Ni mass ratio due to the formation of iron carbide.

Both of these data suggested that in the reduction process of $NiFe_2O_4$, Fe_3O_4 is the first reduction product, followed by the reduction of Ni. With the temperature increases, a rough reduction process of $NiFe_2O_4$ by H_2 and C is $NiFe_2O_4 \rightarrow Fe_3O_4 + NiO \rightarrow Fe_3O_4 + Ni \rightarrow FeO + Fe_xNi_y \rightarrow Fe_xNi_y + Fe$ (or Fe_mC_n). Under the given experimental conditions, this tends to suggest that when using carbon as reductant, metallic Ni could be obtained below 895°C.

3.4 Activation energy for H_2 reduction

Based on the experimental data by using H_2 as reductant, the relationships between $\ln(\beta / T^2)$ and 1/T, as well as reaction mechanism diagrams for the four systems (NiO, Fe_2O_3, $NiFe_2O_4$ and Fe_2O_3 + NiO), are showed in Figs. 9-12, respectively.

The kinetic information for these compounds / systems is summarized in Table 3. The E_a of 87.8 $kJ \cdot mol^{-1}$ of NiO(Fig 9a) was calculated. This value was close to that obtained by Jankovic [5]. And the powder particles used in this experiment had good permeability, and the integral form of the mechanism of NiO was $F(\alpha) = 1 - (1-\alpha)^{1/3}$ [4] (Fig. 9b). Therefore, the rate-controlling step was a phase-boundary-controlled reaction

At the first Fe_2O_3 reduction stage, the E_a of 185.1 $kJ \cdot mol^{-1}$ was obtained (Fig. 10a), which is larger than the value published by Wang et al. [16]. Both the heating rate and reductive degree values used to

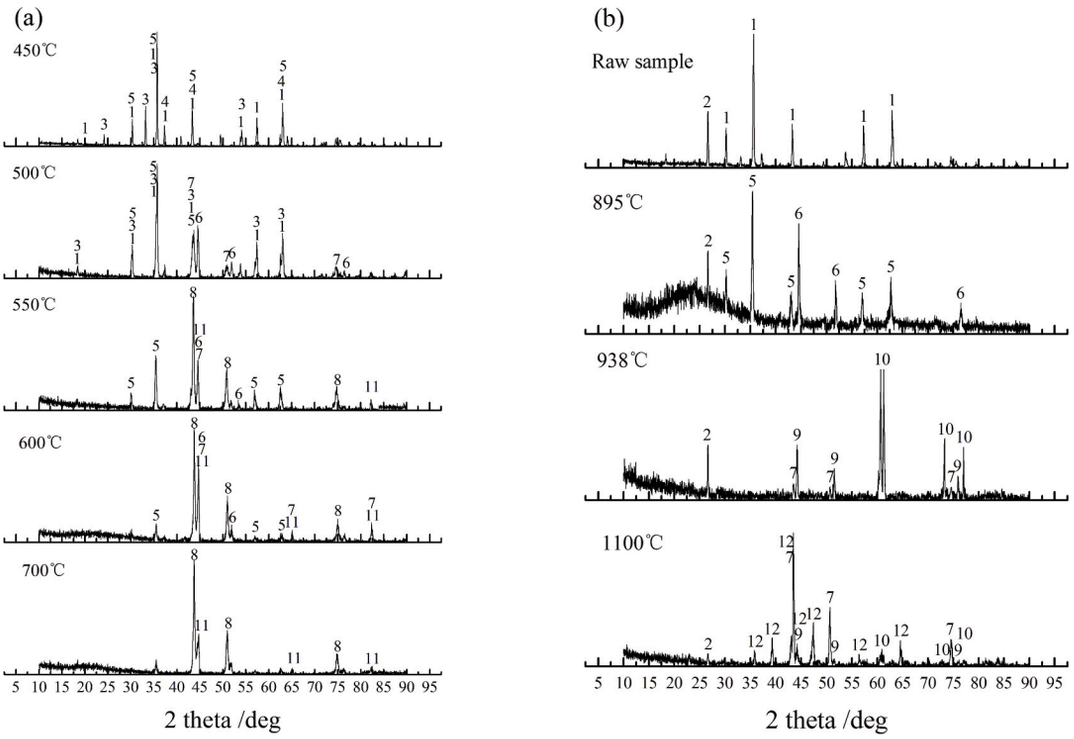

Figure 8. *XRD results: (a: C; b: H_2) (1: $NiFe_2O_4$; 2: C; 3: Fe_2O_3; 4: NiO; 5: Fe_3O_4; 6: Ni; 7: (Fe, Ni); 8: $Fe_{0.64}Ni_{0.36}$; 9: $FeNi_3$; 10: FeO; 11: Fe; 12: Fe_5C_2)*

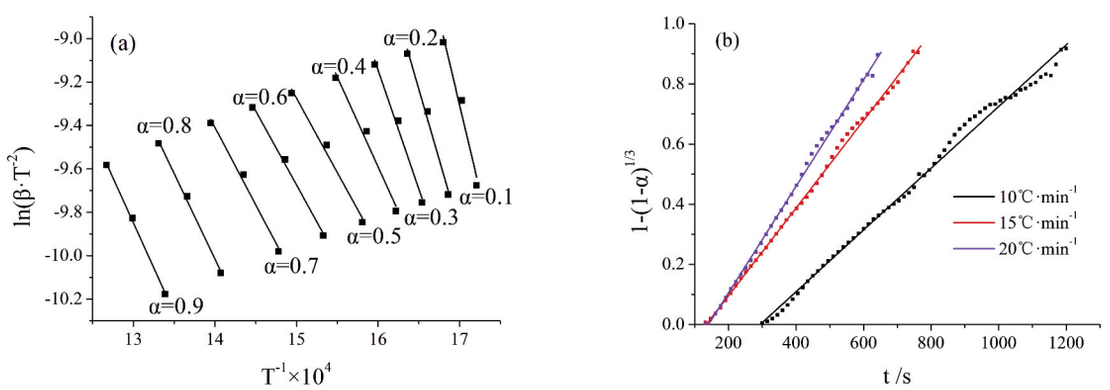

Figure 9. *Arrhenius diagrams (a) and reaction mechanism (b) for NiO*

Table 3. *Reaction parameters and mechanisms of oxide reduction with H_2*

Process	Activation energy ($kJ \cdot min^{-1}$)	Published activation energy ($kJ \cdot min^{-1}$)	The integral form of reaction mechanism	Mechanism
NiO → Ni	87.8	90.8 [4]	$1-(1-\alpha)^{1/3}$	phase-boundary reaction.
$Fe_2O_3 \rightarrow Fe_3O_4$	185.1	107 [13]	$1-(1-\alpha)^{1/3}$	phase-boundary reaction
Fe_3O_4 → Fe	53.8	54 [14]	$[-\ln(1-\alpha)]^{1/4}$	4D formation and growth of nuclei
$NiFe_2O_4$ → Fe/Ni	69.4	62.6 [11]	$\ln[\alpha/(1-\alpha)]$	autocatalytic reaction
Fe_2O_3 + NiO → Fe/Ni	71.3		$1-(1-\alpha)^{1/3}$	phase-boundary reaction and autocatalytic reaction
			$\ln[\alpha/(1-\alpha)]$	

calculate E_a in this paper were small. Therefore, the temperature corresponding to α was relatively low, and the activation energy would be high. Fig. 10b shows the average activation energy was 53.8 kJ·mol^{-1} in the later stage, which was nearly same as the values obtained by Tiernan (54 kJ·mol^{-1}) [14]. As shown in Fig. 10c, the integral form of the mechanism was $F(\alpha)=1-(1-\alpha)^{1/3}$, and the rate-controlling step was a phase-boundary reaction at the first reduction stage of Fe_2O_3. For the second stage, the integral form of the mechanism was $F(\alpha)=[-\ln(1-\alpha)]^{1/4}$ [14], and the rate-controlling step was the 4D formation and growth of nuclei. The phase-boundary reaction and the formation and growth of nuclei controlled the reduction reaction of Fe_2O_3.

The same two kinetic parameters of $NiFe_2O_4$ could be obtained from Fig.11. The E_a was 69.4 kJ·mol^{-1}, which was similar to the value reported in literature [12] (62.6 kJ·mol^{-1}). Good reactivity of powder particles indicates that there is not an obvious boundary between the two stages [12]. The results of tests performed using the resistance furnace and TG prove that the formation of the Fe-Ni alloy was favorable in the reduction reaction. And the integral form of the mechanism was $F(\alpha)=\ln(\frac{\alpha}{1-\alpha})$ [11], so the reaction of $NiFe_2O_4$ with H_2 was an autocatalytic process.

From Fig. 12, the integral form of the mechanism was F(α)=1-(1-α)1/3 at the initial stage. This illustrated that the phase-boundary reaction was the rate-controlling step for the reduction of Fe_2O_3 + NiO.

At the later stage, the form was $F(\alpha)=\ln(\frac{\alpha}{1-\alpha})$ and the reaction was autocatalytic.

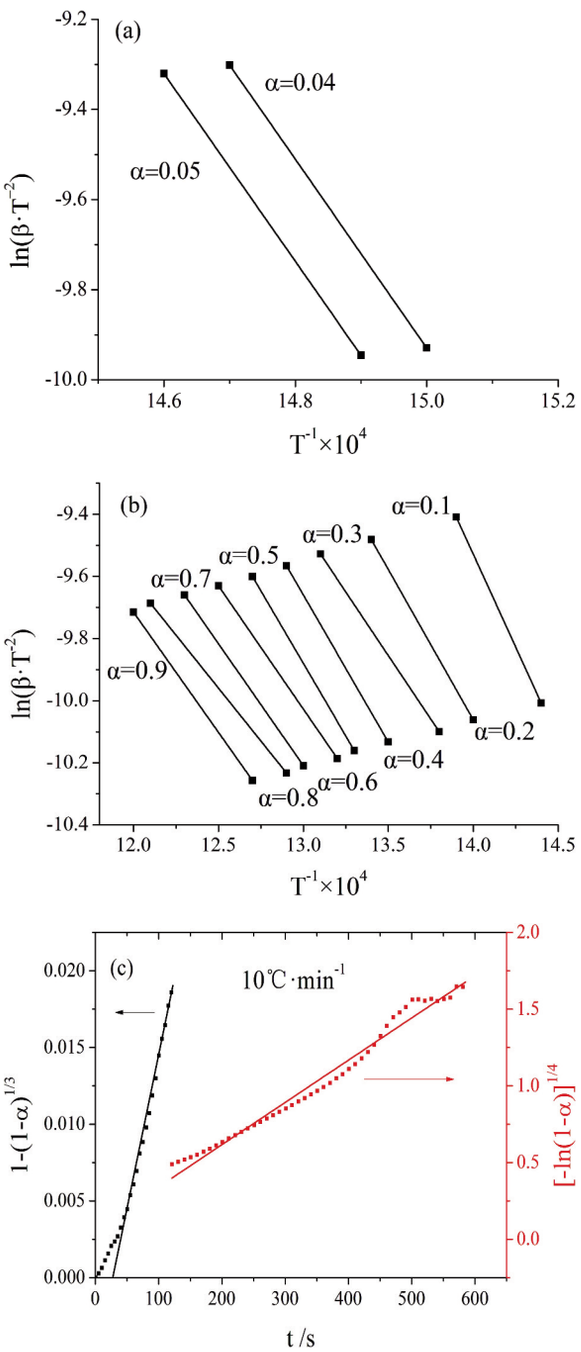

Figure 10. *Arrhenius diagrams for the overall reduction of: (a) hematite to magnetite; (b) magnetite to metallic iron; and (c) reaction mechanism for Fe_2O_3*

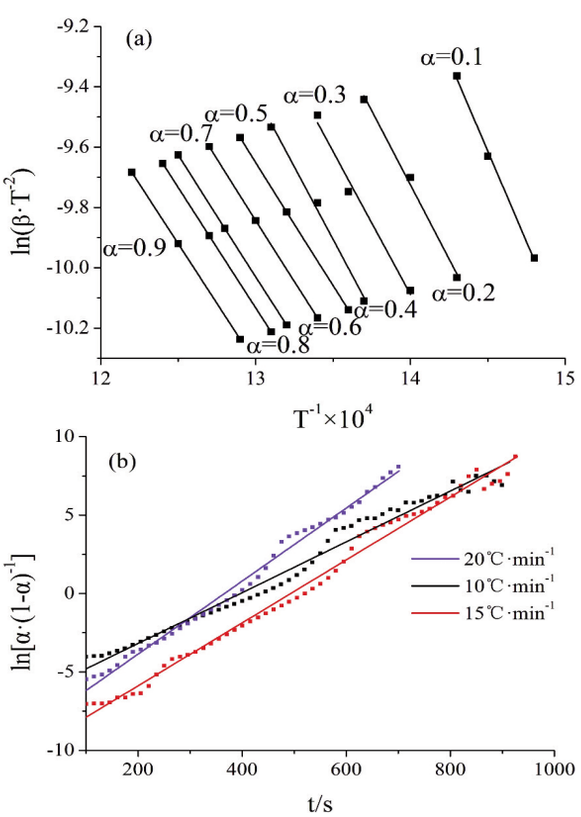

Figure 11. *Arrhenius diagrams (a) and reaction mechanism (b) for $NiFe_2O_4$*

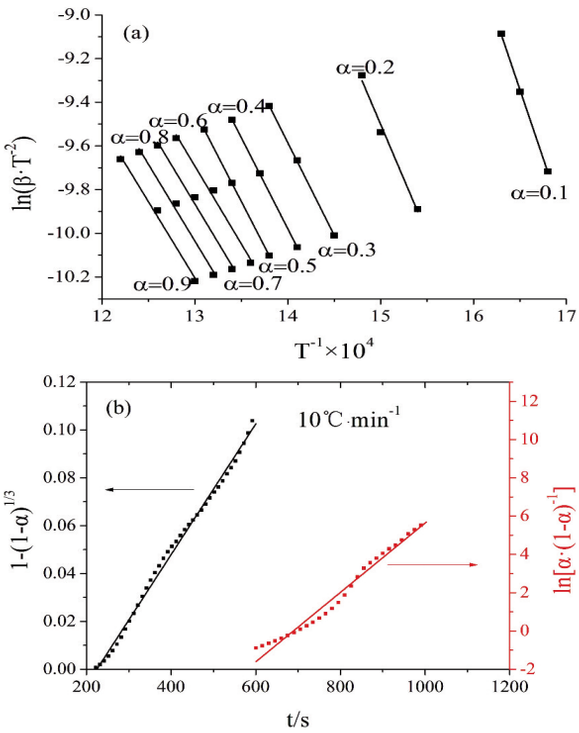

Figure 12. *Arrhenius diagrams (a) and reaction mechanism (b) for Fe_2O_3 + NiO*

4. Conclusions

According to the results in this paper, the following conclusions were obtained:

Compared the case of using H_2 as reductant, all of the five Fe-Ni-O systems showed higher starting reaction temperatures and larger reaction rates during their reductions by C. And, the differences on reduction behaviors by C among these five Fe-Ni-O systems are much larger than using H_2 as reductant.

In the case of C as reductant, the reduction of Fe_2O_3 + NiO system was much easier compared to $NiFe_2O_4$, Fe_2O_3 + Ni, and pure Fe_2O_3. A possible reason is that the heat released from the initial reduction of NiO by CO leads to a higher temperature and better kinetic conditions. In both cases, $NiFe_2O_4$ appeared more difficult to be reduced because it required a higher starting temperature, exhibited a lower reaction rate and lower final reduction degree.

The experimental data suggested that, with increasing temperature, the products for the reduction of $NiFe_2O_4$ appeared in the order $NiFe_2O_4 \rightarrow Fe_3O_4$ + NiO $\rightarrow Fe_3O_4$ + Ni $\rightarrow$ FeO + $Fe_xNi_y \rightarrow Fe_xNi_y$ + Fe (or Fe_mC_n).

From the results of the TG experiments, the activation energies of NiO and $NiFe_2O_4$ were 87.8 kJ·mol^{-1} and 69.4 kJ·mol^{-1}, and the phase-boundary reaction and autocatalytic reaction were the rate-controlling mechanisms, respectively. The reduction path for Fe_2O_3 can be expressed as: $Fe_2O_3 \rightarrow Fe_3O_4 \rightarrow$ Fe. The activation energies were 185.1 kJ·mol^{-1} and 53.8 kJ·mol^{-1}, and the initial rate-controlling step was the phase-boundary reaction, while the 4D formation and growth of nuclei was rate-controlling at the final stage; The activation energy of Fe_2O_3 + NiO was 71.3 kJ·mol^{-1}, and the rate-controlling mechanisms were the phase-boundary reaction and the autocatalytic reaction.

Acknowledgements

This work was financially supported by National Natural Science Foundation of China (No.51074025) and the Fundamental Research Funds for the Central Universities (FRF-SD-12-009A).

References

[1] Ma G J, Fang W, Xu Z H, Xue Z L, Wang W, Sun W H. The Chinese Journal of Process Engineering, 10 (2010) 68-72.

[2] Peng B, Peng J J. North China Univ. of Tech, 15 (2003) 34-40.

[3] Li Y C, Yu C, Wang Q, Li Q J, Hong X. The Chinese Journal of Process Engineering, 10 (6) (2010) 1115-1118.

[4. Wang C Y, Yin F, Chen Y Q, Wang Z, Wang J. The Chinese Journal of Nonferrous Metals, 18 (2008) s1-s8.

[5] Jankovic´ B, Adna Y evic´ B, Mentus S. Chemical Engineering Science, 63 (2008) 567-575.

[6] Sharma S K, Vastola F J, Walker P L. Great Britain, 34 (1996) 1407-1412.

[7] Sharma S K, Vastola F J, Walker P L. Great Britain, 35 (1997) 529-533.

[8] Pineau A, Kannari N, Gaballah I. Thermochimica Acta, 447 (2006) 89-100.

[9] Liu G-S, Strezov V, Lucas J A, Wibberley L J. Thermochimica Acta, 410 (2004) 133-140.

[10] Abdel Halim K S. Materials Science and Engineering A, 452 (1) (2007) 15-22.

[11] Nasr M I, Omar A A, Khedr M H, El-Grassy A A. Scandinavian Journal of Metallurgy, 23 (3) (1994) 119-125.

[12] Hamdy Khedr M. J. Anal. Appl. Pyrolysis, 73(2005) 123-129.

[13] Wei F R, Zhang Y L, et al. The Chinese Journal of Process Engineering, 11(5) (2011): 28-35.

[14] Tiernan M J, Barnes P A, Parkes M B. J. Phys. Chem. B, 105 (2001) 220-228.

[15] Abdel-Halim K S, Khedr M H, Nasr M I, Abdel-Wahab M Sh. Journal of Alloys and Compounds, 463 (2008) 585-590.

[16] Wang H, Yang Y, Wu B-S, Xu J, Ding M-Y, Wang H-L, Fan W-H, Xiang H-W, Li Y-W. Journal of Molecular Catalysis A: Chemical, 308 (2009) 96-107.